Acta Crystallographica Section F
Structural Biology and Crystallization Communications
ISSN 1744-3091

Purification, crystallization and preliminary X-ray analysis of L-sorbose reductase from *Gluconobacter frateurii* complexed with L-sorbose or NADPH

Keiko Kubota,[a] Koji Nagata,[a] Ken-ichi Miyazono,[a] Hirohide Toyama,[b,c] Kazunobu Matsushita[b] and Masaru Tanokura[a]*

[a]Department of Applied Biological Chemistry, Graduate School of Agricultural and Life Sciences, University of Tokyo, 1-1-1 Yayoi, Bunkyo-ku, Tokyo 113-8657, Japan, [b]Department of Biological Chemistry, Faculty of Agriculture, Yamaguchi University, 1677-1 Yoshida, Yamaguchi-shi, Yamaguchi 753-8515, Japan, and [c]Department of Bioscience and Biotechnology, Faculty of Agriculture, University of The Ryukyus, 1 Senbaru, Nishihara-cho, Okinawa 903-0213, Japan

Correspondence e-mail: amtanok@mail.ecc.u-tokyo.ac.jp

Received 30 January 2009
Accepted 20 April 2009

NADPH-dependent L-sorbose reductase (SR) from *Gluconobacter frateurii* was expressed in *Escherichia coli*, purified and crystallized with L-sorbose or NADPH using the sitting-drop vapour-diffusion method at 293 K. Crystals of the SR–L-sorbose complex and the SR–NADPH complex were obtained using reservoir solutions containing PEG 2000 or PEG 400 as precipitants and diffracted X-rays to 2.38 and 1.90 Å resolution, respectively. The crystal of the SR–L-sorbose complex belonged to space group $C222_1$, with unit-cell parameters a = 124.2, b = 124.1, c = 60.8 Å. The crystal of the SR–NADPH complex belonged to space group $P2_1$, with unit-cell parameters a = 124.3, b = 61.0, c = 124.5 Å, β = 89.99°. The crystals contained two and eight molecules, respectively, in the asymmetric unit.

1. Introduction

L-Sorbose reductase (SR; EC 1.1.1.289) from the acetic acid bacterium *Gluconobacter frateurii* is an NADPH-dependent oxidoreductase that belongs to the short-chain dehydrogenase/reductase (SDR) family. SR catalyzes the oxidoreduction between L-sorbose and D-sorbitol (Soemphol *et al.*, 2007) and only utilizes L-sorbose and D-sorbitol as substrates with high specificity. In contrast, the substrate specificities of other SDR-family proteins that are able to utilize L-sorbose are generally low: SOU1 from *Candida albicans* (Greenberg *et al.*, 2005), aldehyde reductase from *Galdieria sulphuraria* (Gross *et al.*, 1997) and L-iditol 2-dehydrogenase from *Rhodobacter sphaeroides* (Philippsen *et al.*, 2005) catalyze the reduction of L-sorbose to D-sorbitol, L-sorbitol and L-iditol, respectively, but these proteins also use other sugars and sugar alcohols as substrates. The high substrate specificity of SR is a unique characteristic among SDR-family enzymes. In addition, SR is thought to play a critical role in L-sorbose metabolism in *G. frateurii* because disruption of the SR gene results in a significant growth reduction under L-sorbose-rich conditions (Soemphol *et al.*, 2007). Structure determination of SR would reveal the unique substrate-recognition mechanism of SR that distinguishes it from general SDR-family enzymes. Here, we report the expression, purification, crystallization and preliminary X-ray analysis of L-sorbose reductase from *G. frateurii* complexed with L-sorbose or NADPH.

2. Materials and results

2.1. Overexpression and purification

A gene fragment including the SR gene (GenBank code AB192961; *sboA*) was amplified by PCR and cloned into the *Hin*dIII/*Not*I site of pET-28a(+) plasmid (Novagen). Although the gene fragment was cloned into the *Hin*dIII/*Not*I site of pET-28a(+), the expression construct was designed to overexpress only SR protein (residues 1–263), because the amplified fragment includes the SR gene and its upstream sequence from *G. frateurii* that contains a ribosome-binding site. SR was overexpressed in *Escherichia coli* BL21 (DE3) cells (Novagen) harbouring the constructed plasmid. The expression of SR was induced by the addition of 0.5 m*M* (final

concentration) isopropyl β-D-1-thiogalactopyranoside (IPTG) when the optical density of the medium at 600 nm reached 1.3. The cells were further cultivated for 4 h at 303 K to accumulate the target protein. The harvested cells were resuspended in 10 m*M* MES buffer pH 6.0 containing 1 m*M* EDTA and 10% glycerol (MEG buffer) and then disrupted by sonication. After centrifugation at 40 000*g* for 30 min, the supernatant was applied onto a Resource Q (GE Healthcare) column pre-equilibrated with MEG buffer and SR was eluted with a linear gradient of 0–0.2 *M* NaCl. The fractions containing SR were pooled and dialyzed against MEG buffer supplemented with 1.2 *M* ammonium sulfate. The sample was applied onto a Resource PHE (GE Healthcare) column pre-equilibrated with MEG buffer supplemented with 1.2 *M* ammonium sulfate. SR was eluted with a linear gradient of 1.2–0 *M* ammonium sulfate. The sample was finally applied onto a Superdex 200 (GE Healthcare) column pre-equilibrated with MEG buffer supplemented with 150 m*M* NaCl. All purification procedures were performed at 277 K.

2.2. Crystallization

The purified SR was dialyzed against 10 m*M* MES buffer pH 6.2 supplemented with 5 m*M* TCEP (trisphosphine hydrochloride; Pierce) and concentrated to 15 mg ml^{-1}. For the cocrystallization of SR with its substrate or cofactor, final concentrations of 10 m*M* L-sorbose or 5 m*M* NADPH were added to the protein solution. All crystallization experiments were performed at 293 K using the sitting-drop vapour-diffusion method.

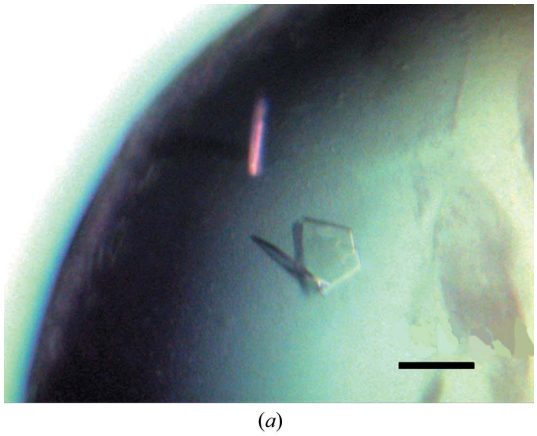

(*a*)

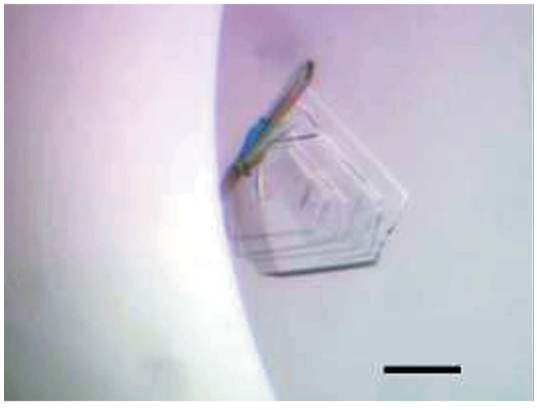

(*b*)

Figure 1
Crystals of SR complexed with (*a*) L-sorbose and (*b*) NADPH. The scale bars are 100 µm in length.

Initial crystallization screening of the SR–L-sorbose complex and SR–NADPH complex were carried out with the screening kits Crystal Screen HT (Hampton Research) and Wizard I, II and III (Emerald BioSystems). After refinement of the crystallization conditions, the best crystal of the SR–L-sorbose complex was obtained by mixing 1.0 µl SR–L-sorbose solution and 1.0 µl reservoir solution consisting of 32%(*w*/*v*) PEG 2000 and 100 m*M* sodium acetate trihydrate pH 5.0 (Fig. 1*a*). For cryoprotection, the crystal of

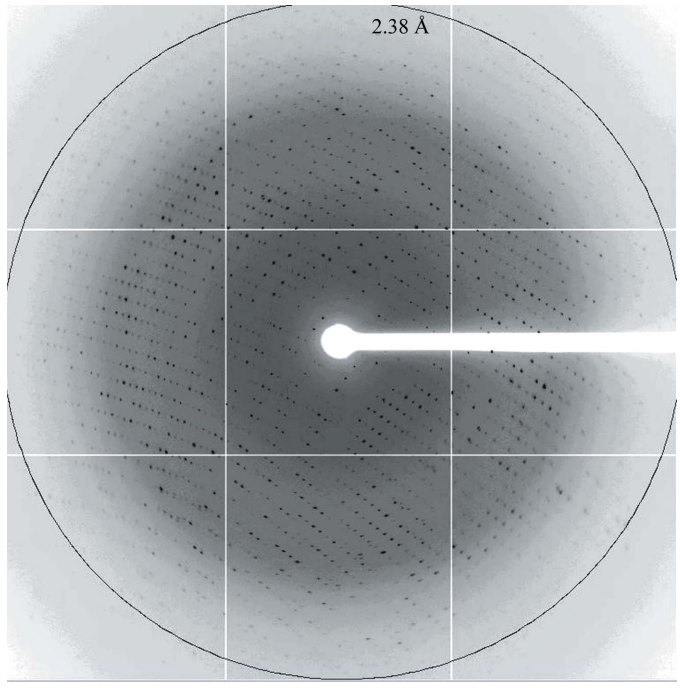

(*a*)

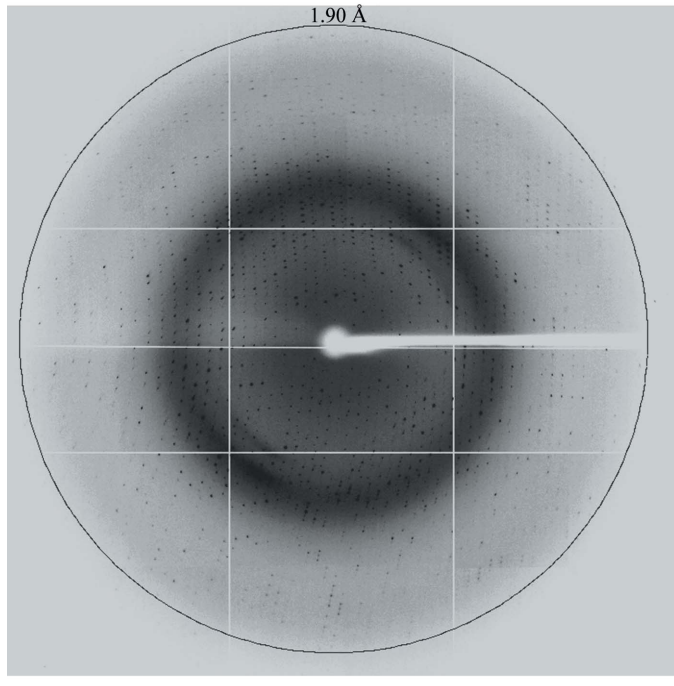

(*b*)

Figure 2
X-ray diffraction images of (*a*) the SR–L-sorbose complex crystal and (*b*) the SR–NADPH complex crystal. The circles display resolutions of (*a*) 2.38 Å and (*b*) 1.90 Å.

Table 1
Summary of data-collection statistics of SR crystals.

Values in parentheses are for the highest resolution shell.

	SR–L-sorbose complex	SR–NADPH complex
Beamline	SPring-8 BL41XU	PF BL5A
Wavelength (Å)	1.000	1.000
Space group	$C222_1$	$P2_1$
Unit-cell parameters		
a (Å)	124.2	124.3
b (Å)	124.1	61.0
c (Å)	60.9	124.5
β (°)		89.99
Resolution (Å)	50.0–2.38 (2.47–2.38)	50.0–1.9 (1.95–1.90)
No. of measurements	242012	545146
No. of unique reflections	19391	146936
Completeness (%)	99.9 (99.7)	99.7 (99.8)
$R_{\rm merge}$†	0.094 (0.338)	0.070 (0.383)
$\langle I\rangle/\langle\sigma(I)\rangle$	34.0 (5.1)	11.1 (3.4)

† $R_{\rm merge} = \sum_{hkl}\sum_i |I_i(hkl) - \langle I(hkl)\rangle|/\sum_{hkl}\sum_i I_i(hkl)$, where $I_i(hkl)$ is the ith intensity measurement of reflection hkl, including symmetry-related reflections, and $\langle I(hkl)\rangle$ is its average.

the SR–L-sorbose complex was soaked in reservoir solution supplemented with 20%(*v*/*v*) ethylene glycol for a few seconds. The best crystal of the SR–NADPH complex was obtained by mixing 1.0 µl SR–NADPH solution and 1.0 µl reservoir solution consisting of 34%(*w*/*v*) PEG 400, 200 m*M* calcium acetate and 100 m*M* sodium acetate trihydrate pH 4.5 (Fig. 1*b*). Both crystals were mounted on cryoloops and flash-cooled at 100 K in a nitrogen stream for data collection.

2.3. Data collection and processing

The X-ray diffraction data set for the SR–L-sorbose complex was collected on the BL41XU beamline at SPring-8 (Harima, Japan) using an ADSC Quantum 315 CCD detector (Fig. 2*a*). The best crystal of the SR–L-sorbose complex diffracted X-rays to 2.38 Å resolution. The diffraction data were indexed, integrated and scaled with *HKL*-2000 (Otwinowski & Minor, 1997). The crystal of the SR–L-sorbose complex was found to belong to the *C*-centred orthorhombic space group $C222_1$, with unit-cell parameters a = 124.2, b = 124.1, c = 60.8 Å. The crystal contained two molecules of SR in the asymmetric unit, with a solvent content of 40.6% according to the Matthews coefficient calculation (Matthews, 1968).

The X-ray diffraction data set for the SR–NADPH complex was collected on the BL5A beamline at the Photon Factory (Tsukuba, Japan) using an ADSC Quantum 315 CCD detector (Fig. 2*b*). The best crystal of the SR–NADPH complex diffracted X-rays to 1.90 Å resolution. The diffraction data were indexed, integrated and scaled with *XDS* (Kabsch, 1993). The crystal of the SR–NADPH complex belonged to the primitive monoclinic space group $P2_1$, with unit-cell parameters a = 124.3, b = 61.0, c = 124.5 Å, β = 89.99°. Although the unit-cell parameters of the SR–NADPH complex seemed to indicate a tetragonal or orthorhombic space group, we could not scale the data set in these space groups: the $R_{\rm merge}$ values of the data set became significantly worse (approximately 40% for all data), suggesting that the crystal of the SR–NADPH complex may have pseudosymmetry. The crystal contained eight molecules in the asymmetric unit, with a solvent content of 41.0% (Matthews, 1968). Data-collection statistics for each crystal are provided in Table 1.

The crystal structures were determined by the molecular-replacement method. Initial models of the SR–L-sorbose complex and the SR–NADPH complex were determined using *MOLREP* (Vagin & Teplyakov, 1997) with the coordinates of 1-phenylethanol dehydrogenase (PDB code 2ew8; Höffken *et al.*, 2006), which shares the highest amino-acid sequence similarity with SR among proteins for which structures have been determined, as a template model. Initial R factors from *MOLREP* were 0.540 and 0.799 and the correlation coefficients were 0.366 and 0.376, respectively. Several cycles of refinement using *REFMAC*5 (Murshudov *et al.*, 1997) resulted in the $R/R_{\rm free}$ values of 0.391/0.523 and 0.440/0.476, respectively. Further refinement and model building are in progress.

We are grateful to the staff members at beamline BL41XU at SPring-8 (Harima, Japan; 2006A-2721-NL1-np-P3k) and at BL5A at Photon Factory (Tsukuba, Japan; 2008G139). This work was supported in part by the National Project on Protein Structural and Functional Analyses and the Targeted Proteins Research Program (TPRP) of the Ministry of Education, Culture, Sports, Science and Technology, Japan.

References

Greenberg, J., Price, N., Oliver, R., Sherman, F. & Rustchenko, E. (2005). *Yeast*, **22**, 957–969.
Gross, W., Seipold, P. & Schnarrenberger, C. (1997). *Plant Physiol.* **114**, 231–236.
Höffken, H., Duong, M., Friedrich, T., Breuer, M., Hauer, B., Reinhardt, R., Rabus, R. & Heider, J. (2006). *Biochemistry*, **45**, 82–93.
Kabsch, W. (1993). *J. Appl. Cryst.* **26**, 795–800.
Matthews, B. W. (1968). *J. Mol. Biol.* **33**, 491–497.
Murshudov, G. N., Vagin, A. A. & Dodson, E. J. (1997). *Acta Cryst.* D**53**, 240–255.
Otwinowski, Z. & Minor, W. (1997). *Methods Enzymol.* **276**, 307–326.
Philippsen, A., Schirmer, T., Stein, M. A., Giffhorn, F. & Stetefeld, J. (2005). *Acta Cryst.* D**61**, 374–379.
Soemphol, W., Toyama, H., Moonmangmee, D., Adachi, O. & Matsushita, K. (2007). *J. Bacteriol.* **189**, 4800–4808.
Vagin, A. & Teplyakov, A. (1997). *J. Appl. Cryst.* **30**, 1022–1025.